

# A Comparison of Upwind Difference Schemes for Compressible Flows of Ideal and Non-Ideal Gases in a Duct

P. Glaister

Department of Mathematics and Statistics, PO Box 220  
University of Reading, Reading RG6 6AX, UK

## Abstract

In a recent paper [1] a number of numerical schemes were presented for the Euler equations governing compressible flows of an ideal gas in a duct of variable cross section, the principal one of which is based on a conservative linearisation approach. This scheme was subsequently extended to encompass compressible duct flows of real gases where the equation of state allows for non-ideal gases [2]. These schemes use different parameter vectors in their construction and, consequently, the scheme in [2] when applied to the special case of an ideal gas is not identical to the principal ideal gas scheme in [1]. The schemes also vary as to whether the source term arising out of the geometry of the problem is handled using upwinding or treated as a point source. In this paper a numerical comparison of these schemes is made when each is applied to a standard test problem for the ideal gas case.

**Mathematics Subject Classification:** 65M06, 35L65, 76L05

**Keywords:** Euler equations, ideal and non-ideal gases, duct flows

## 1 Introduction

In a recent paper [1] a number of numerical schemes were presented for the Euler equations governing compressible flows of an ideal gas in a duct of variable cross section, including the case of cylindrical symmetry. The principal scheme in [1] is based on a conservative linearisation approach and utilized a parameter vector which included the pressure variable. This scheme was subsequently extended to encompass compressible duct flows of real gases where the equation of state allows for non-ideal gases [2], but it was noted that, when

applied to the special case of an ideal gas, gave rise to different averaging of the flow variables, and a different source term, because the specific internal energy was used in the parameter vector to allow for easier handling in the non-ideal case.

In this paper we seek to compare these two schemes when applied to a problem involving reflection and interaction of a converging cylindrical shock. This will also include the effect of handling the source term arising out of the variable geometry by upwinding or as a point source.

## 2 The Governing Equations

The unsteady ‘one-dimensional’ Euler equations governing the compressible flow of a real gas can be written in conservation form as

$$\underline{u}_t + \underline{f}_r = \underline{s} \quad , \quad (2.1)$$

where

$$\underline{u} = (\rho, \rho u, e)^T \quad (2.2)$$

are the conserved variables, and the flux function

$$\underline{f}(\underline{u}) = (\rho u, p + \rho u^2, u(e + p))^T \quad , \quad (2.3)$$

together with

$$e = \rho i + \frac{1}{2} \rho u^2 \quad (2.4)$$

and the ‘source’ term

$$\underline{s}(\underline{u}) = -\frac{S'(r)}{S(r)} (\rho u, \rho u^2, u(e + p))^T \quad . \quad (2.5)$$

The quantities  $(\rho, u, p, i, e) = (\rho, u, p, i, e)(r, t)$  represent the density, velocity, pressure, specific internal energy and total energy of the fluid, respectively, at a general position  $r$  along a duct, of cross-sectional area  $S(r)$ , and at time  $t$ . The particular case  $S(r) = r^N$  represents slab symmetry ( $N = 0$ ), cylindrical symmetry ( $N = 1$ ) or spherical symmetry ( $N = 2$ ), with the coordinate  $r$  being given by  $r = x$ ,  $r = \sqrt{x^2 + y^2}$  or  $r = \sqrt{x^2 + y^2 + z^2}$ , respectively, where  $x, y, z$  represent Cartesian coordinates. In addition, there is an equation of state relating the pressure, density and specific internal energy of the form

$$p = p(\rho, i) \quad . \quad (2.6)$$

For future reference, the quasi-linear form of equation (2.1) is given by

$$\underline{u}_t + A\underline{u}_r = \underline{s} \quad , \quad (2.7)$$

where the Jacobian of the flux function  $\underline{f}$  is given by

$$A = \underline{f}_{\underline{u}} = \begin{pmatrix} 0 & 1 & 0 \\ a^2 - u^2 - \frac{p_i}{\rho} \left( \frac{p}{\rho} + i - \frac{1}{2}u^2 \right) & 2u - u \frac{p_i}{\rho} & \frac{p_i}{\rho} \\ ua^2 - u \left( \frac{p}{\rho} + i + \frac{1}{2}u^2 \right) & \frac{p}{\rho} + i + \frac{1}{2}u^2 - u^2 \frac{p_i}{\rho} & u + u \frac{p_i}{\rho} \\ -u \frac{p_i}{\rho} \left( \frac{p}{\rho} + i - \frac{1}{2}u^2 \right) & & \end{pmatrix} \quad (2.8)$$

and where the sound speed,  $a$ , is given by

$$a^2 = p_\rho + \frac{pp_i}{\rho^2} . \quad (2.9)$$

In the special case of an ideal gas the equation of state (2.6) is given by

$$p = (\gamma - 1)\rho i \quad , \quad (2.10)$$

where the constant  $\gamma$  denotes the ratio of specific heat capacities of the gas, and the sound speed in (2.9) becomes

$$a^2 = \frac{\gamma p}{\rho} \quad , \quad (2.11)$$

with the Jacobian (2.8) simplifying to

$$A = \underline{f}_{\underline{u}} = \begin{pmatrix} 0 & 1 & 0 \\ \frac{(\gamma-3)}{2}u^2 & (3-\gamma)u & \gamma-1 \\ \frac{(\gamma-2)}{2}u^3 - \frac{ua^2}{\gamma-1} & \frac{(3-2\gamma)}{2}u^2 + \frac{a^2}{\gamma-1} & \gamma u \end{pmatrix} . \quad (2.12)$$

### 3 Conservative Linearisation

In both [1] and [2] the schemes are based on a conservative linearisation approach, which we now describe in brief.

For a given cell  $C$  in the numerical grid, define a flux balance

$$\underline{\Phi} = - \int_C \underline{f}_r dr = -[\underline{f}]_L^R = -(f(\underline{u}_R) - f(\underline{u}_L)) = -\Delta \underline{f} \quad , \quad (3.1)$$

denoting the change in flux balance across the boundaries of the cell. The numerical approximation to  $\underline{\Phi}$  is defined to be of the form

$$\widehat{\underline{\Phi}} = -\Delta r \widehat{\underline{f}}_r = -\Delta r \widehat{A} \widehat{\underline{u}}_r \quad , \quad (3.2)$$

where  $\Delta r$  is the cell length and  $\hat{\bullet}$  indicates a discretised quantity. Having determined the precise form for  $\hat{\Phi}$ , which we describe shortly, the distribution of the flux balance to the nodes at either end of the cell is then made using upwinding. Conservation requires that the overall contribution to the nodes depends only on the boundary conditions. Thus, for a linearisation represented by (3.2) to be conservative, the sum over the computational domain of the  $\hat{\Phi}$  should reduce to boundary conditions alone. It follows from (3.1) that a linearisation is conservative if  $\hat{\Phi} = \Phi$  for each cell, and the resulting scheme is conservative provided all of the discrete flux balance is distributed to the nodes of the grid.

## 4 Numerical Schemes

Simple linearisations of the Euler equations can be achieved by seeking discrete Jacobians  $\hat{A}$  in (3.2) which allow  $\hat{\Phi}$  to be easily decomposed into components and then an application of the upwinding technique is made. By evaluating the Jacobian consistently from some average cell state  $\bar{z}$ , so that

$$\hat{A} = \underline{f}_{\underline{u}}(\bar{z}) = A(\bar{z}) \quad (4.1)$$

and then assume that the components of a parameter vector vary linearly in space within each cell. An important consequence of the linear variation is that  $\underline{z}_r$  is locally constant and so the conservative flux balance can be written as

$$\Phi = - \int_C \underline{f}_r dr = - \int_C \underline{f}_{\underline{z}} \underline{z}_r dr = - \left( \int_C \underline{f}_{\underline{z}} dr \right) \underline{z}_r \quad (4.2)$$

A conservative linearisation is then given by

$$\hat{\Phi} = - \left( \int_C \underline{f}_{\underline{z}} dr \right) \bar{z}_r \quad (4.3)$$

where the corresponding discrete gradient (evaluated under the assumption of linearly varying  $\underline{z}$ ) is given by

$$\bar{z}_r = \frac{\underline{z}_R - \underline{z}_L}{\Delta r} = \frac{\Delta \underline{z}}{\Delta r} \quad (4.4)$$

It follows that the discrete gradient of the conservative variables can be written as

$$\bar{u}_r = \frac{1}{\Delta r} \int_C \underline{u}_r dr = \frac{1}{\Delta r} \int_C \underline{u}_{\underline{z}} \underline{z}_r dr = \frac{1}{\Delta r} \left( \int_C \underline{u}_{\underline{z}} dr \right) \bar{z}_r \quad (4.5)$$

and thus, from (4.3) and (4.5), the discrete conservative flux balance is given by

$$\hat{\Phi} = \hat{\Phi}_{\underline{z}} = -\Delta r \left( \int_C \underline{f}_{\underline{z}} dr \right) \left( \int_C \underline{u}_{\underline{z}} dr \right)^{-1} \bar{u}_r \quad (4.6)$$

Thus the discrete conservative flux balance (3.2) is given by (4.6) in which  $\widehat{\underline{u}}_r = \overline{\underline{u}}_r$  and

$$\widehat{A} = \widehat{A}_{\underline{z}} = \left( \int_C \underline{f}_{\underline{z}} dr \right) \left( \int_C \underline{u}_{\underline{z}} dr \right)^{-1} . \quad (4.7)$$

#### 4.1 Scheme 1 - ideal gas scheme

The principal scheme in [1] for the ideal gas case is based on the parameter vector

$$\underline{z} = \underline{z}_1 = (\rho, u, p)^T , \quad (4.8)$$

and using the overbar  $\overline{\phantom{x}}$  to indicate the consistent evaluation of a quantity solely derived from the cell-average state given by

$$\overline{\underline{z}} = \frac{1}{2}(\underline{z}_L + \underline{z}_R) , \quad (4.9)$$

has

$$\widehat{A}_{\underline{z}_1} = A(\overline{\underline{z}}_1) + K_{\underline{z}_1} , \quad (4.10)$$

where the matrices

$$A(\overline{\underline{z}}_1) = \begin{pmatrix} 0 & 1 & 0 \\ \frac{(\gamma-3)\overline{u}^2}{2} & (3-\gamma)\overline{u} & \gamma-1 \\ \frac{(\gamma-2)\overline{u}^3}{2} - \frac{\gamma\overline{p}\overline{u}}{(\gamma-1)\overline{p}} & \frac{(3-2\gamma)\overline{u}^2}{2} + \frac{\gamma\overline{p}}{(\gamma-1)\overline{p}} & \gamma\overline{u} \end{pmatrix} \quad (4.11)$$

and

$$K_{\underline{z}_1} = \begin{pmatrix} 0 & 0 & 0 \\ \frac{(3-\gamma)(\Delta u)^2}{24} + \frac{(\gamma-3)\overline{u}\Delta\rho\Delta u}{12\overline{p}} & -\frac{(\gamma-3)\Delta\rho\Delta u}{12\overline{p}} & 0 \\ \frac{(\gamma-3)\overline{u}^2\Delta\rho\Delta u}{12\overline{p}} - \frac{\gamma\overline{u}(\Delta u)^2}{24} & \frac{(\Delta u)^2}{8} - \frac{(\gamma-3)\overline{u}\Delta\rho\Delta u}{12\overline{p}} & 0 \end{pmatrix} . \quad (4.12)$$

(See [1] for a derivation of this.) The flux balance in (4.6) can then be written as

$$\widehat{\underline{\Phi}}_{\underline{z}_1} = -\Delta r (A(\overline{\underline{z}}_1) + K_{\underline{z}_1}) \overline{\underline{u}}_r = \overline{\underline{\Phi}}_{\underline{z}_1} + \underline{q}_{\underline{z}_1} , \quad (4.13)$$

where that part of the flux balance:

$$\overline{\underline{\Phi}}_{\underline{z}_1} = -\Delta r A(\overline{\underline{z}}_1) \overline{\underline{u}}_r \quad (4.14)$$

is handled in the usual upwinding sense, and using  $\Delta r \underline{u}_r = \Delta \underline{u}$ , together with

$$\Delta(\rho u) = \bar{\rho} \Delta u + \bar{u} \Delta \rho \quad , \quad (4.15)$$

the term  $q_{\underline{z}_1}$  in (4.13) can be simplified as

$$q_{\underline{z}_1} = -\Delta r K_{\underline{z}_1} \underline{u}_r = \begin{pmatrix} 0 \\ \frac{(\gamma-3)}{8} \Delta \rho (\Delta u)^2 \\ \frac{(\gamma-3)}{8} \bar{u} \Delta \rho (\Delta u)^2 - \frac{1}{8} \bar{\rho} (\Delta u)^3 \end{pmatrix} \quad , \quad (4.16)$$

which is treated as a 'source' and is expected to be negligible in smooth flows, but to have an effect at discontinuities. The gradient  $\underline{u}_r$  in (4.14) is projected onto the local eigenvectors of  $A(\underline{z}_1)$ , for which the eigenvalues and eigenvectors are

$$\lambda_i(\underline{z}_1) = \bar{u} \pm \hat{a}, \bar{u} \quad , \quad (4.17a-c)$$

$$\underline{e}_i(\underline{z}_1) = \left( 1, \bar{u} \pm \hat{a}, \frac{\hat{a}^2}{\gamma-1} + \frac{1}{2} \bar{u}^2 \pm \bar{u} \hat{a}^2 \right)^T \quad , \quad (1, \bar{u}, \frac{1}{2} \bar{u}^2)^T \quad , \quad (4.18a-c)$$

where

$$\hat{a} = \sqrt{\frac{\gamma \bar{p}}{\bar{\rho}}} = \sqrt{\frac{\gamma(p_L + p_R)}{(\rho_L + \rho_R)}} \quad , \quad (4.19)$$

representing approximations to the continuous values

$$\lambda_i = u \pm a, \quad u, \underline{e}_i = \left( 1, u \pm a, \frac{a^2}{\gamma-1} + \frac{1}{2} u^2 \pm ua \right)^T \quad , \quad (1, u, \frac{1}{2} u^2)^T \quad , \quad a = \sqrt{\frac{\gamma p}{\rho}} \quad . \quad (4.20a-g)$$

## 4.2 Scheme 2 - real gas scheme applied to ideal gases

The principal scheme in [2] which allows for the non-ideal case is based on the parameter vector

$$\underline{z} = \underline{z}_2 = (\rho, u, i)^T \quad , \quad (4.21)$$

where the specific internal energy,  $i$ , is used instead of the pressure,  $p$ , and using the same notation in §4.1, has

$$\hat{A}_{\underline{z}_2} = A(\underline{z}_2) + K_{\underline{z}_2} \quad , \quad (4.22)$$

where the matrices

$$A(\bar{z}_2) = \begin{pmatrix} 0 & 1 & 0 \\ -\frac{p_i(\bar{\rho}, \bar{i})}{\bar{\rho}} \left( \frac{p(\bar{\rho}, \bar{i})}{\bar{\rho}} + \bar{i} - \frac{1}{2}\bar{u}^2 \right) & 2\bar{u} - \bar{u} \frac{p_i(\bar{\rho}, \bar{i})}{\bar{\rho}} & \frac{p_i(\bar{\rho}, \bar{i})}{\bar{\rho}} \\ \bar{u} \tilde{a}^2 - \bar{u} \left( \frac{p(\bar{\rho}, \bar{i})}{\bar{\rho}} + \bar{i} + \frac{1}{2}\bar{u}^2 \right) & \frac{p(\bar{\rho}, \bar{i})}{\bar{\rho}} + \bar{i} + \frac{1}{2}\bar{u}^2 - \bar{u}^2 \frac{p_i(\bar{\rho}, \bar{i})}{\bar{\rho}} & \bar{u} + \bar{u} \frac{p_i(\bar{\rho}, \bar{i})}{\bar{\rho}} \\ -\bar{u} \frac{p_i(\bar{\rho}, \bar{i})}{\bar{\rho}} \left( \frac{p(\bar{\rho}, \bar{i})}{\bar{\rho}} + \bar{i} - \frac{1}{2}\bar{u}^2 \right) & & \end{pmatrix} \quad (4.23)$$

and

$$K_{z_2} = \begin{pmatrix} 0 & 0 & 0 \\ \frac{(\Delta u)^2}{12} - \frac{\bar{u} \Delta \rho \Delta u}{12 \bar{\rho}} + \frac{p_i}{\bar{\rho}} \left( \frac{\bar{u} \Delta \rho \Delta u}{12 \bar{\rho}} - \frac{(\Delta u)^2}{24} \right) & \frac{\Delta \rho \Delta u}{6 \bar{\rho}} - \frac{p_i \Delta \rho \Delta u}{12 \bar{\rho}^2} & 0 \\ \Delta \rho \Delta u \left( -\frac{u^2}{8 \bar{\rho}} - \frac{\bar{i}}{12 \bar{\rho}} - \frac{\bar{u}^2 p_{\rho i}}{24 \bar{\rho}} + \frac{p_{\rho \rho}}{12} + \frac{\bar{u}^2 p_i}{12 \bar{\rho}^2} - \frac{\bar{i} p_{\rho i}}{12 \bar{\rho}} \right) & \frac{p_{\rho \rho} (\Delta \rho)^2}{24 \bar{\rho}} - \frac{\bar{u} p_{ii} \Delta u \Delta i}{12 \bar{\rho}} + \frac{p_{ii} (\Delta i)^2}{24 \bar{\rho}} + \frac{p_{\rho i} \Delta \rho \Delta i}{12 \bar{\rho}} + \frac{\bar{u} \Delta \rho \Delta u}{12 \bar{\rho}} + \frac{(\Delta u)^2}{8} & \frac{\Delta \rho \Delta u}{12 \bar{\rho}} + \frac{p_{\rho i} \Delta \rho \Delta u}{12 \bar{\rho}} \\ -\frac{\bar{u} \Delta \rho \Delta i}{12 \bar{\rho}} - \frac{\bar{u} p_{\rho \rho} (\Delta \rho)^2}{24 \bar{\rho}} - \frac{\bar{u} p_{ii} (\Delta i)^2}{24 \bar{\rho}} & -\frac{\bar{u} p_{\rho i} \Delta \rho \Delta u}{12 \bar{\rho}} - \frac{\bar{u} p_i \Delta \rho \Delta u}{12 \bar{\rho}^2} + \frac{\Delta \rho \Delta i}{12 \bar{\rho}} \\ -(\Delta u)^2 \left( \frac{\bar{u}}{24} + \frac{\bar{u} p_i}{24 \bar{\rho}} \right) & & \end{pmatrix},$$

+ higher order terms

(4.24)

where all derivatives of  $p$  are evaluated at  $(\bar{\rho}, \bar{i})$ , and where we have denoted

$$\tilde{a}^2 = p_\rho(\bar{\rho}, \bar{i}) + \frac{p(\bar{\rho}, \bar{i}) p_i(\bar{\rho}, \bar{i})}{\bar{\rho}^2}. \quad (4.25)$$

(See [2] for a derivation of this.) The flux balance in (4.6) can then be written as

$$\widehat{\Phi}_{z_2} = -\Delta r (A(\bar{z}_2) + K_{z_2}) \bar{u}_r = \bar{\Phi}_{z_2} + \underline{q}_{z_2}, \quad (4.26)$$

where, as for the scheme in §4.1, that part of the flux balance:

$$\bar{\Phi}_{z_2} = -\Delta r A(\bar{z}_2) \bar{u}_r \quad (4.27)$$

is handled in the usual upwinding sense, the term

$$\underline{q}_{\underline{z}_2} = -\Delta r K_{\underline{z}_2} \underline{u}_r \tag{4.28}$$

is treated as a 'source', and is again expected to be negligible in smooth flows, but to have an effect at discontinuities. The gradient  $\underline{u}_r$  in (4.27) is again projected onto the local eigenvectors of  $A(\underline{z}_2)$ , for which the eigenvalues and eigenvectors are

$$\lambda_i(\underline{z}_2) = \bar{u} \pm \tilde{a}, \bar{u} \quad , \tag{4.29a-c}$$

$$\underline{e}_i(\underline{z}_2) = \left( 1, \bar{u} \pm \tilde{a}, \frac{p(\bar{\rho}, \bar{i})}{\bar{\rho}} + \bar{i} + \frac{1}{2}\bar{u}^2 \pm \bar{u}\tilde{a} \right)^T, \quad \left( 1, \bar{u}, \bar{i} + \frac{1}{2}\bar{u}^2 - \frac{\bar{\rho}p_{\rho}(\bar{\rho}, \bar{i})}{p_i(\bar{\rho}, \bar{i})} \right)^T \quad . \tag{4.30a-c}$$

These represent approximations to the continuous values

$$\lambda_i = u \pm a, \quad u \quad , \quad \underline{e}_{1,2} = \left( 1, u \pm a, \frac{p}{\rho} + i + \frac{1}{2}u^2 \pm ua \right)^T \quad , \tag{4.31a-g}$$

$$\underline{e}_3 = \left( 1, u, i + \frac{1}{2}u^2 - \frac{pp_{\rho}}{p_i} \right)^T, \quad a = \sqrt{p_{\rho} + \frac{pp_i}{\rho^2}} \quad .$$

In the special case of an ideal gas given by (2.10) the higher order terms in (4.24) vanish, together with  $p_{\rho i} \equiv \gamma - 1$ ,  $p_{\rho\rho}, p_{ii} \equiv 0$ , and

$$\begin{aligned} p(\bar{\rho}, \bar{i}) &= (\gamma - 1)\bar{\rho}\bar{i}, \quad p_{\rho}(\bar{\rho}, \bar{i}) = (\gamma - 1)\bar{i} \\ p_i(\bar{\rho}, \bar{i}) &= (\gamma - 1)\bar{\rho}, \quad \tilde{a}^2 = \gamma(\gamma - 1)\bar{i} \end{aligned} \quad , \tag{4.32a-d}$$

so that matrices in (4.23) and (4.24) become

$$\begin{aligned} A(\underline{z}_2) &= \begin{pmatrix} 0 & 1 & 0 \\ \frac{(\gamma-3)\bar{u}^2}{2} & (3-\gamma)\bar{u} & \gamma-1 \\ \frac{(\gamma-2)\bar{u}^3}{2} - \gamma\bar{u}\bar{i} & \frac{(3-2\gamma)\bar{u}^2}{2} + \gamma\bar{i} & \gamma\bar{u} \end{pmatrix} \\ &= \begin{pmatrix} 0 & 1 & 0 \\ \frac{(\gamma-3)\bar{u}^2}{2} & (3-\gamma)\bar{u} & \gamma-1 \\ \frac{(\gamma-2)\bar{u}^3}{2} - \frac{\bar{u}\tilde{a}^2}{\gamma-1} & \frac{(3-2\gamma)\bar{u}^2}{2} + \frac{\tilde{a}^2}{\gamma-1} & \gamma\bar{u} \end{pmatrix} \end{aligned} \tag{4.33}$$



and

$$K_{\bar{z}_2} = \begin{pmatrix} 0 & 0 & 0 \\ \frac{(\gamma-3)\bar{u}\Delta\rho\Delta u}{12\bar{\rho}} - \frac{(\gamma-3)(\Delta u)^2}{24} & -\frac{(\gamma-3)\Delta\rho\Delta u}{12\bar{\rho}} & 0 \\ \frac{\gamma\Delta u\Delta i}{12} - \frac{\gamma\Delta\rho(\Delta u)^3}{288\bar{\rho}} - \frac{\gamma\bar{u}(\Delta u)^2}{24} - \frac{\gamma\bar{u}\Delta\rho\Delta i}{12\bar{\rho}} & \frac{(\Delta u)^2}{8} + \frac{(3-2\gamma)\bar{u}\Delta\rho\Delta u}{12\bar{\rho}} & \frac{\gamma\Delta\rho\Delta u}{12\bar{\rho}} \\ -\frac{\gamma\bar{i}\Delta\rho\Delta u}{12\bar{\rho}} + \frac{(\gamma-2)\bar{u}^2\Delta\rho\Delta u}{8\bar{\rho}} + \frac{\gamma\bar{u}(\Delta\rho\Delta u)^2}{144\bar{\rho}^2} & +\frac{\gamma\Delta\rho\Delta i}{12\bar{\rho}} - \frac{\gamma(\Delta\rho\Delta u)^2}{144\bar{\rho}^2} & \frac{\gamma\Delta\rho\Delta u}{12\bar{\rho}} \end{pmatrix}, \quad (4.34)$$

where

$$\tilde{a}^2 = \gamma(\gamma-1)\bar{i} = \gamma\left(\frac{p}{\rho}\right) = \gamma\frac{1}{2}\left(\frac{p_L}{\rho_L} + \frac{p_R}{\rho_R}\right). \quad (4.35)$$

Therefore, in this special case, the flux balance in (4.26) can be written as

$$\hat{\Phi}_{\bar{z}_2} = -\Delta r(A(\bar{z}_2) + K_{\bar{z}_2})\bar{u}_r = \bar{\Phi}_{\bar{z}_2} + \underline{q}_{\bar{z}_2}, \quad (4.36)$$

where the matrices  $A(\bar{z}_2)$  and  $K_{\bar{z}_2}$  are given by (4.33) and (4.34). The source term  $\underline{q}_{\bar{z}_2}$  in (4.36) can be simplified as

$$\underline{q}_{\bar{z}_2} = -\Delta r K_{\bar{z}_2} \bar{u}_r = \begin{pmatrix} 0 \\ \frac{(\gamma-3)}{8}\Delta\rho(\Delta u)^2 \\ \frac{(\gamma-3)\bar{u}\Delta\rho(\Delta u)^2}{8} - \frac{1}{8}\bar{\rho}(\Delta u)^3 \\ -\frac{\gamma}{4}\Delta\rho\Delta u\Delta i \end{pmatrix}, \quad (4.37)$$

using  $\Delta r \bar{u}_r = \Delta \underline{u}$  and (4.15), together with

$$\Delta(\rho i) = \bar{\rho}\Delta i + \bar{i}\Delta\rho, \quad (4.38)$$

$$\Delta(\rho u^2) = \bar{u}^2\Delta\rho + 2\bar{\rho}\bar{u}\Delta u + \frac{1}{4}\Delta\rho(\Delta u)^2. \quad (4.39)$$

The eigenvalues and eigenvectors of  $A(\bar{z}_2)$  in (4.29a)-(4.30c) also simplify to

$$\lambda_i(\bar{z}_2) = \bar{u} \pm \tilde{a}, \bar{u}, \quad (4.40a-c)$$

$$\underline{e}_i(\bar{z}_2) = \left(1, \bar{u} \pm \tilde{a}, \frac{\tilde{a}^2}{\gamma-1} + \frac{1}{2}\bar{u}^2 \pm \bar{u}\tilde{a}\right)^T, \quad \left(1, \bar{u}, \frac{1}{2}\bar{u}^2\right)^T, \quad (4.41a-c)$$

again representing approximations to the continuous values in (4.20a-g) in the ideal gas case.

## 5 Source Term

Having considered the treatment of the flux associated with  $\underline{f}$  in (2.1), we now turn to the handling the source term  $\underline{s}$  in (2.5), which can be written as

$$\underline{s}(\underline{u}) = -\frac{S'(r)}{S(r)}(\rho u, \rho u^2, u(e+p))^T = -\frac{S'(r)}{S(r)}\rho u(1, u, H)^T, \quad (5.1)$$

where the enthalpy,  $H$ , is given by

$$H = \frac{e+p}{\rho} = \frac{p}{\rho} + i + \frac{1}{2}u^2, \quad (5.2)$$

using (2.4), and which appears in the first two eigenvectors of  $A$ . A corresponding approximation for the contribution from the source in (5.1) can be made, depending on whether **Scheme 1** or **Scheme 2** is used, as follows.

### 5.1 Scheme 1 - ideal gas scheme

In this case the enthalpy,  $H$ , in (5.2) is given by

$$H = \frac{e+p}{\rho} = \frac{\gamma p}{\rho(\gamma-1)} + \frac{1}{2}u^2 \quad (5.3)$$

using (2.10). In this case we take the additional contribution, due to  $\underline{s}$ , for the update to the solution at time  $t + \Delta t$  in cell  $C$  in the numerical grid as

$$-\Delta t \frac{\Delta S}{\tilde{S}} \bar{\rho} \bar{u} (1, \bar{u}, \tilde{H})^T \quad (5.4)$$

where

$$\tilde{H} = \frac{\tilde{a}^2}{\gamma-1} + \frac{1}{2}\bar{u}^2 = \frac{\gamma \bar{p}}{(\gamma-1)} + \frac{1}{2}\bar{u}^2 \quad (5.5)$$

and  $\tilde{S}$  is an average of  $S$  in the cell.

### 5.2 Scheme 2 - real gas scheme applied to ideal gases

In the real gas case the corresponding approximation to that in (5.4) will be

$$-\Delta t \frac{\Delta S}{\tilde{S}} \bar{\rho} \bar{u} (1, \bar{u}, \tilde{H})^T \quad (5.6)$$

where

$$\tilde{H} = \frac{p(\bar{\rho}, \bar{i})}{\bar{\rho}} + \bar{i} + \frac{1}{2}\bar{u}^2 \quad (5.7)$$

and  $\tilde{S}$  is again an average of  $S$  in the cell. When applied to the ideal gas case (5.7) simplifies to

$$\tilde{H} = \frac{\tilde{a}^2}{\gamma-1} + \frac{1}{2}\bar{u}^2 = \frac{\gamma(\bar{p})}{\gamma-1} + \frac{1}{2}\bar{u}^2 \quad (5.8)$$

using (4.32a) and (4.35), and  $\tilde{S}$  is again an average of  $S$  in the cell.

### 5.3 Distribution of source

Finally, the source terms in (5.4), (5.5) or (5.6), (5.8), depending on which scheme is used, can then either be ‘upwinded’ by projecting onto the local eigenvectors, which are given by (4.18a-c) for **Scheme 1** and (4.41a-c) for **Scheme 2**, or they can be distributed essentially as a point source. Thus, when the source is upwinded in **Scheme 1** we refer to it as **Scheme 1a**, whereas if the source is handled point-wise we refer to it as **Scheme 1b**. We refer as **Scheme 2a** and **Scheme 2b** similarly.

## 6 Test Problem

This problem is concerned with a converging cylindrical shock. We consider a region  $0 \leq r \leq 200$  for the cylindrically symmetric case with  $S(r) = r$  and with  $\gamma = 1.4$ . Initially a cylindrical diaphragm of radius  $r = 100$  separates two uniform regions of gas at rest with initial data in the inner and outer regions as follows:

$$(\rho, u, p) = \begin{cases} 1, 0, 1 & \text{for } 0 \leq r \leq 100 \\ 4, 0, 4 & \text{for } 100 < r \leq 200 \end{cases}$$

When  $t = 0$  the diaphragm is removed and a converging shock wave, followed by a converging contact discontinuity, moves towards the axis,  $r = 0$ , and a diverging rarefaction wave moves outwards. The shock accelerates as it approaches the axis of symmetry, is reflected from the axis and interacts with the contact discontinuity (still converging), which results in a transmitted shock, a converging contact discontinuity, and a weak converging reflected shock.

## 7 Numerical Results

Figures 1-3 show the approximate solution for the density  $\rho$  at times  $t = 50, 80$  and 110 obtained using 200 mesh points with the ideal gas scheme with the source term handled using upwinding, namely **Scheme 1a**, and Figures 4-6 show the corresponding results for **Scheme 1b** when the source term is handled point-wise. The corresponding results using the **Scheme 2a** and **Scheme 2b** designed for real gases and applied to the ideal gas are shown in Figures 7-9 and 10-12, respectively. In all cases the formation of the features, the reflection, interaction and transmission of the shocks and contact discontinuities, and the resulting weak converging shock, can clearly be seen. We also see that the results are comparable across all four schemes in both a qualitative and quantitative sense.

## 8 Conclusions

All four schemes presented produce good results for a problem involving the interaction and reflection of a converging cylindrical shock. Further, these comparable results are achieved regardless of whether the source term arising out of the variable geometry is handled using upwinding or treated in a point-wise sense. This also demonstrates that the use of different averaging of the flow variables, resulting from the ideal gas scheme and the real gas scheme applied to the ideal gas case, has no effect on the quality or accuracy of the solution.

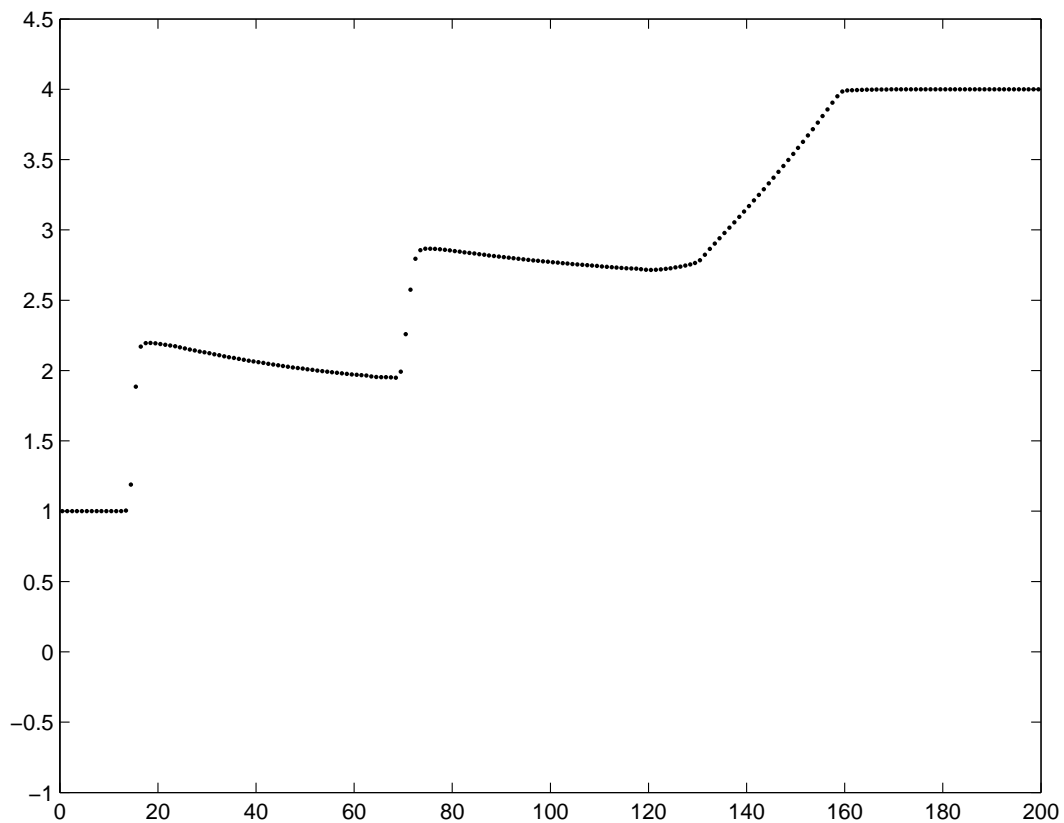


Figure 1: Solution for  $\rho$  using Scheme 1a when  $t = 50$

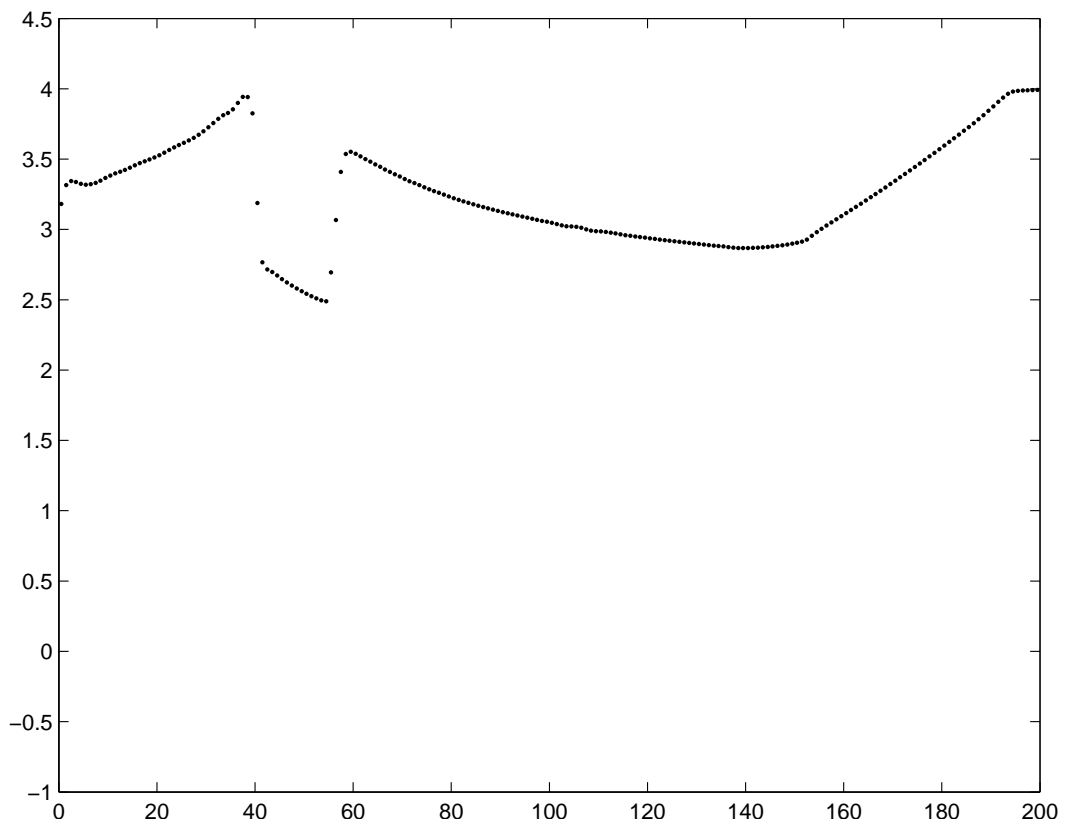


Figure 2: Solution for  $\rho$  using Scheme 1a when  $t = 80$

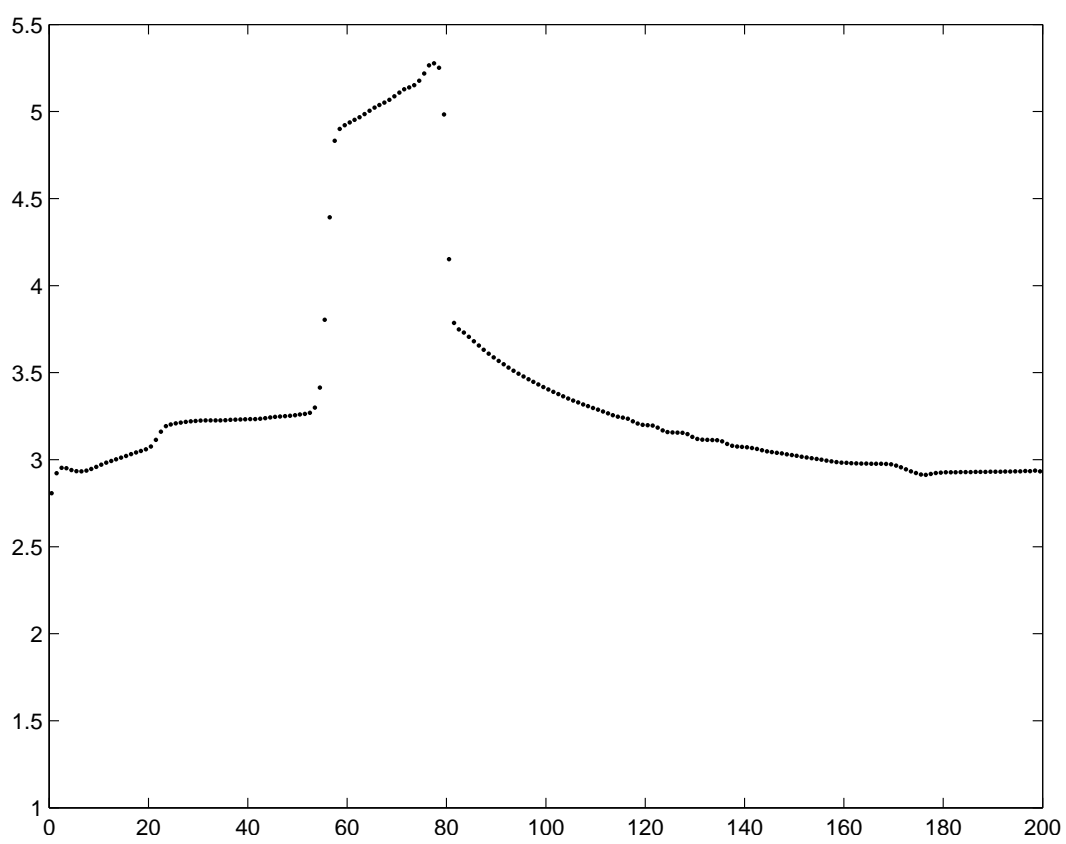


Figure 3: Solution for  $\rho$  using Scheme 1a when  $t = 110$

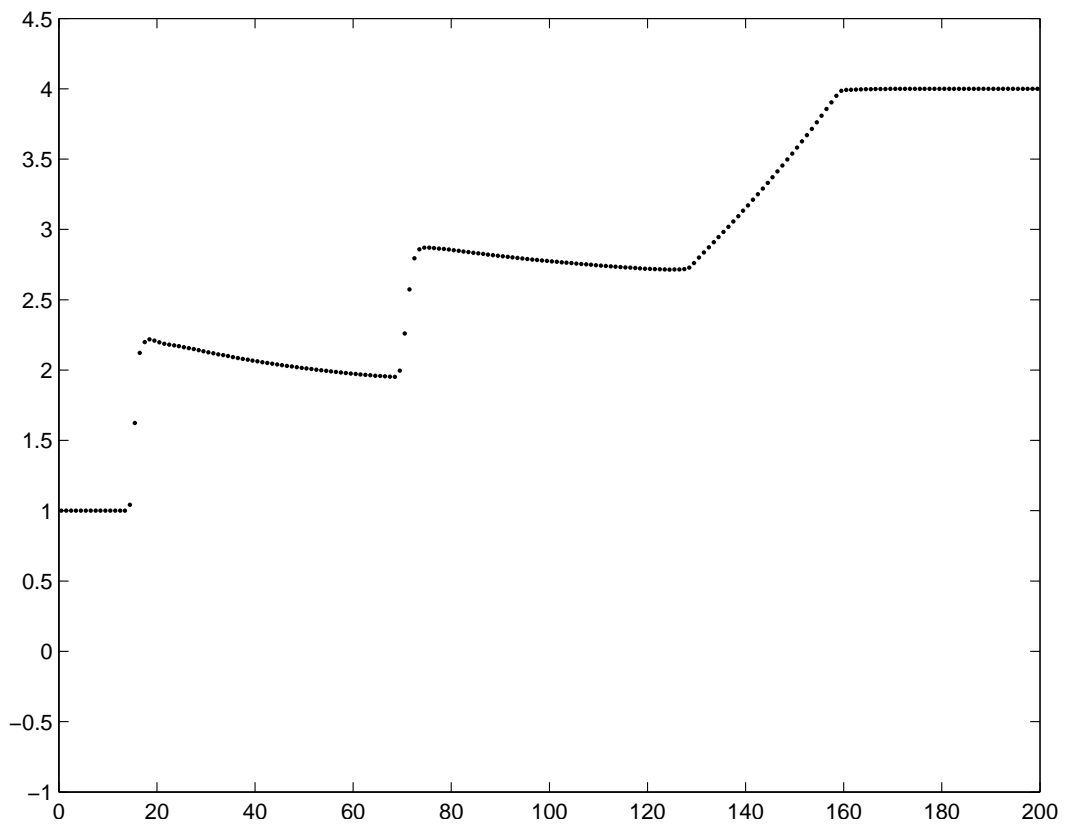


Figure 4: Solution for  $\rho$  using Scheme 1b when  $t = 50$

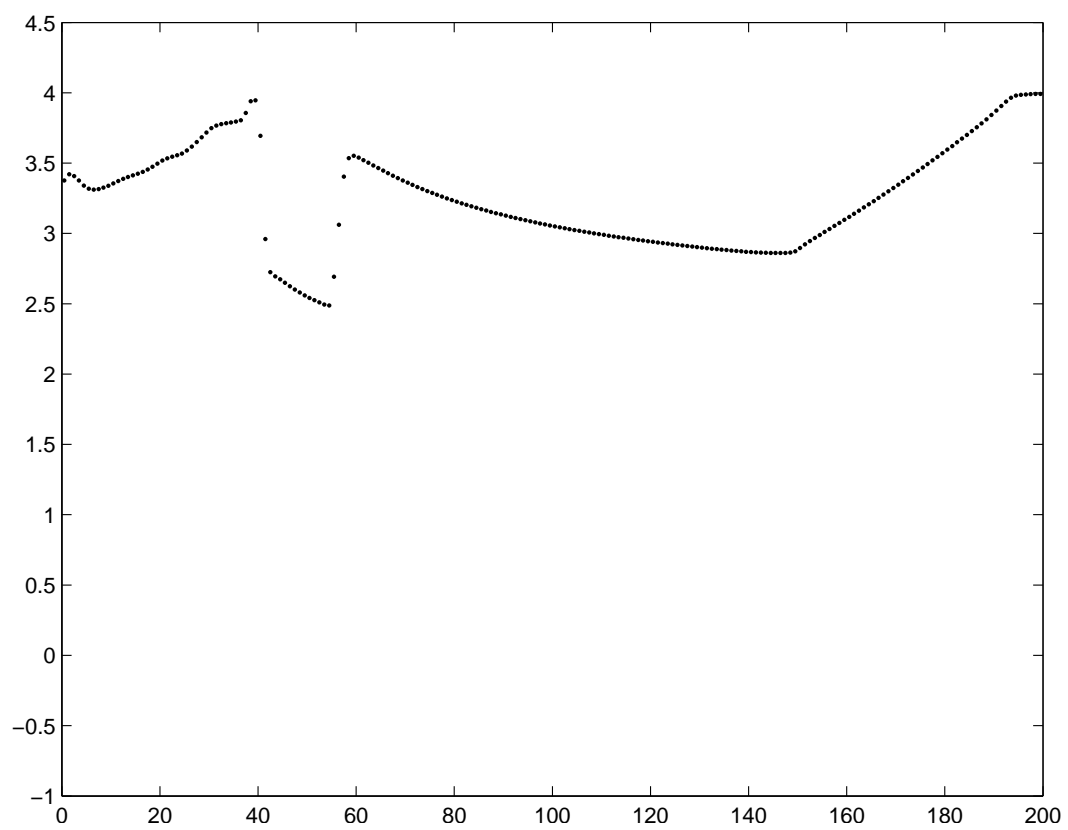


Figure 5: Solution for  $\rho$  using Scheme 1b when  $t = 80$



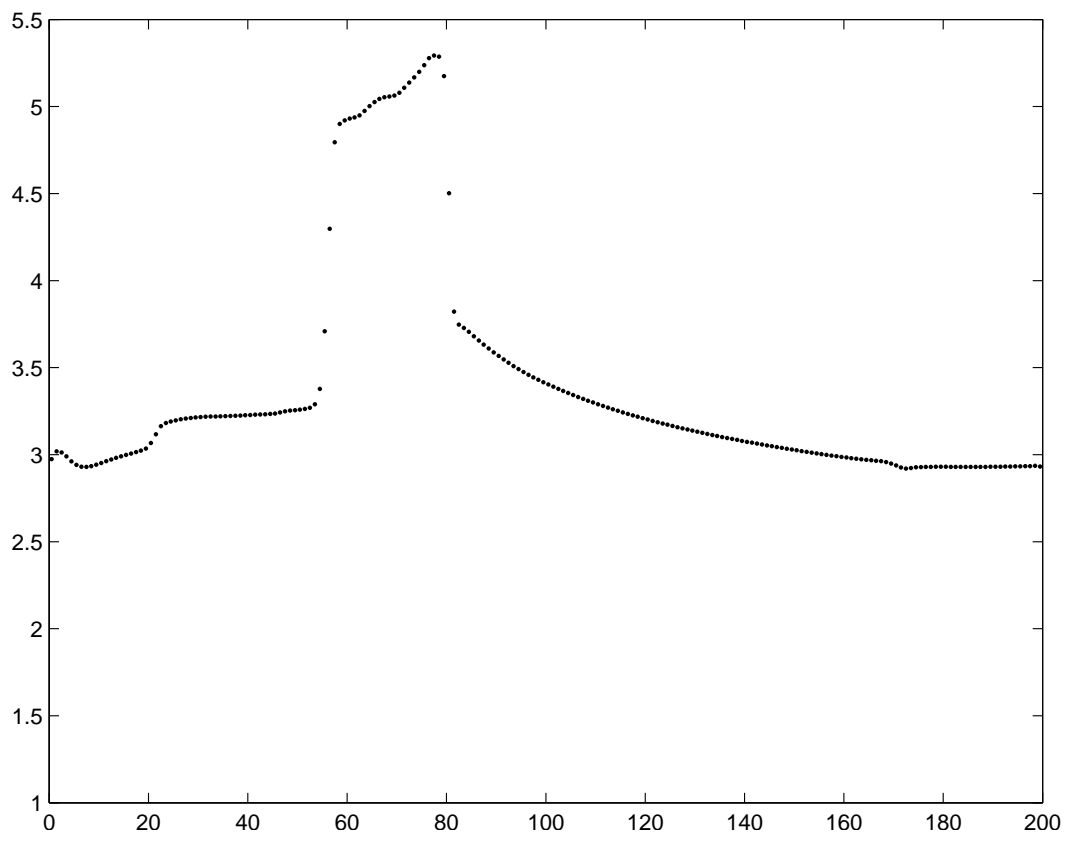


Figure 6: Solution for  $\rho$  using Scheme 1b when  $t = 110$

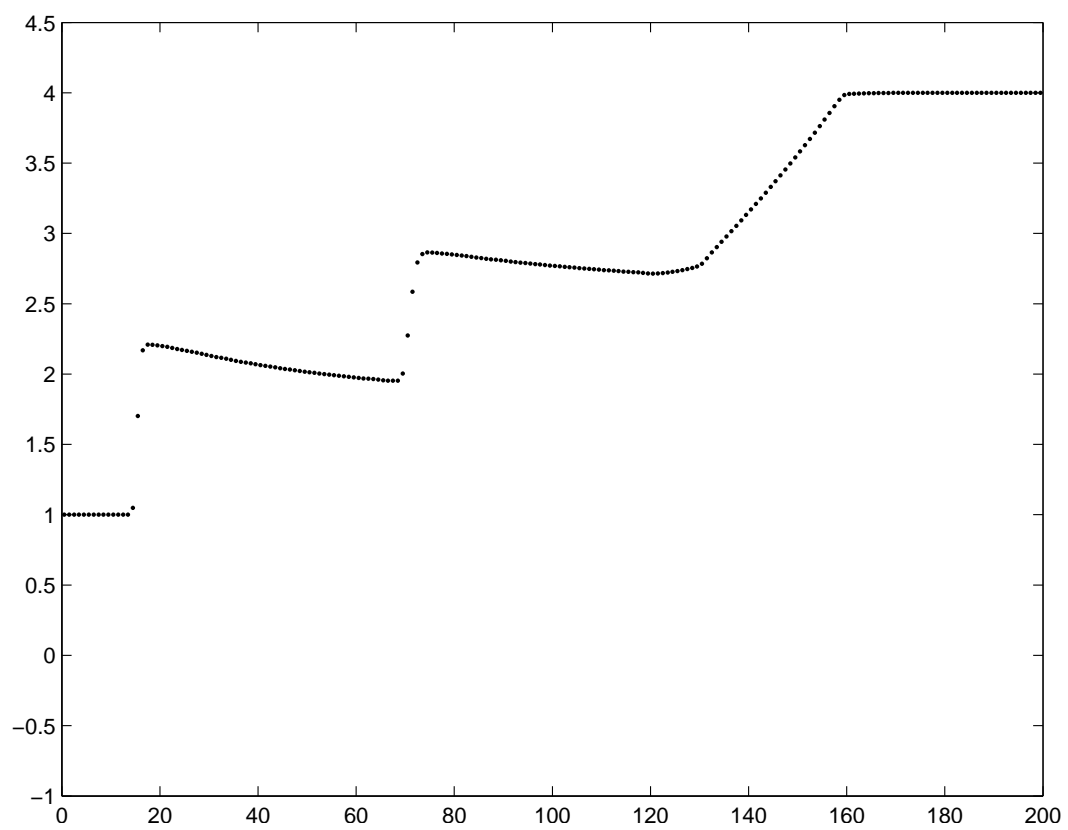


Figure 7: Solution for  $\rho$  using Scheme 2a when  $t = 50$

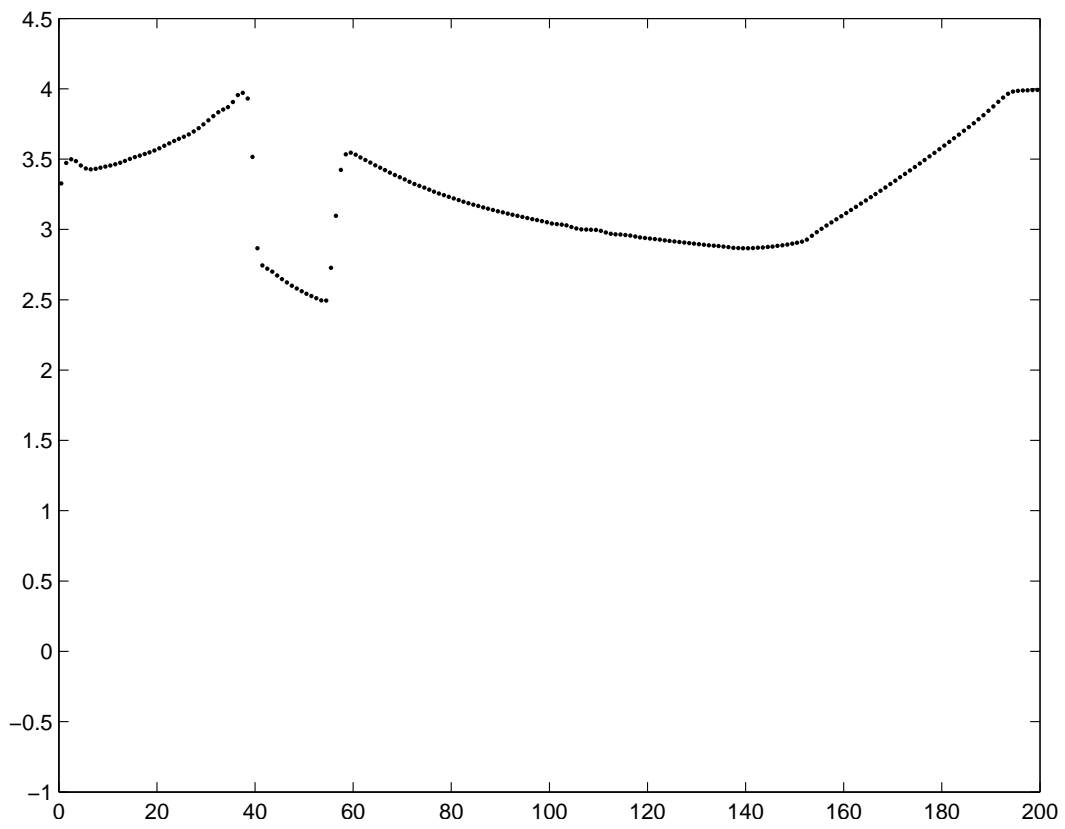


Figure 8: Solution for  $\rho$  using Scheme 2a when  $t = 80$

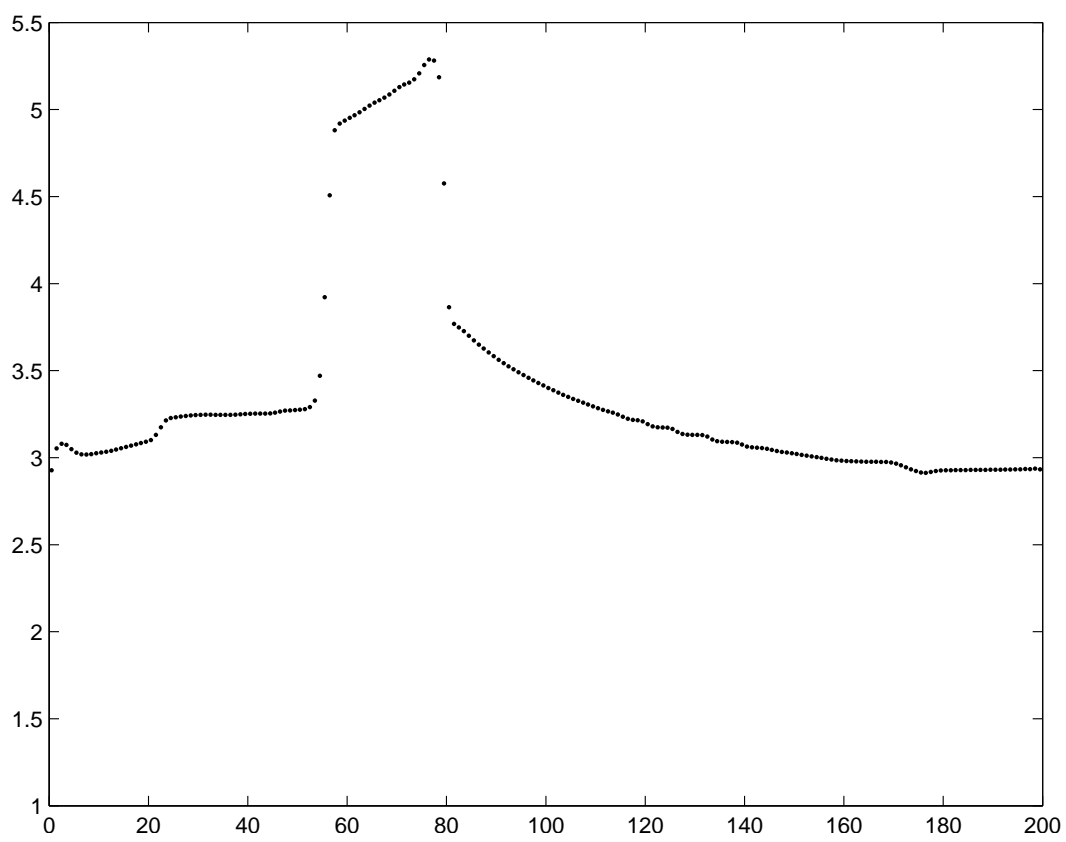


Figure 9: Solution for  $\rho$  using Scheme 2a when  $t = 110$

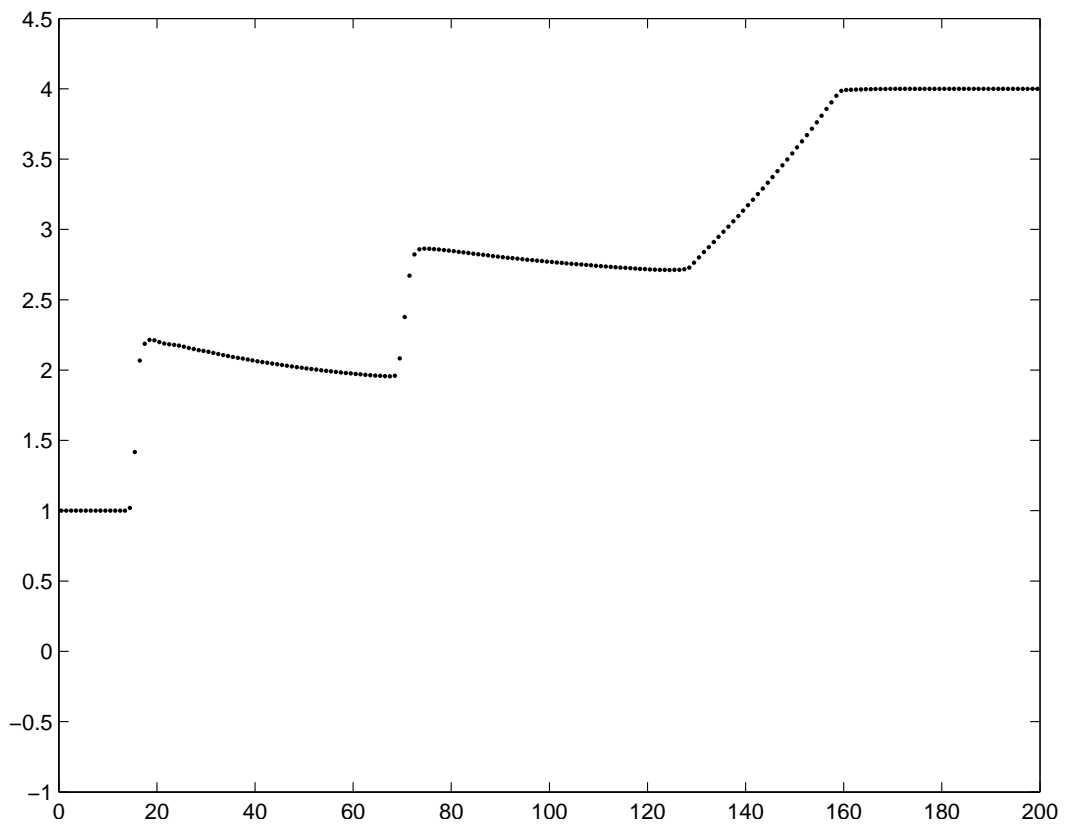


Figure 10: Solution for  $\rho$  using Scheme 2b when  $t = 50$

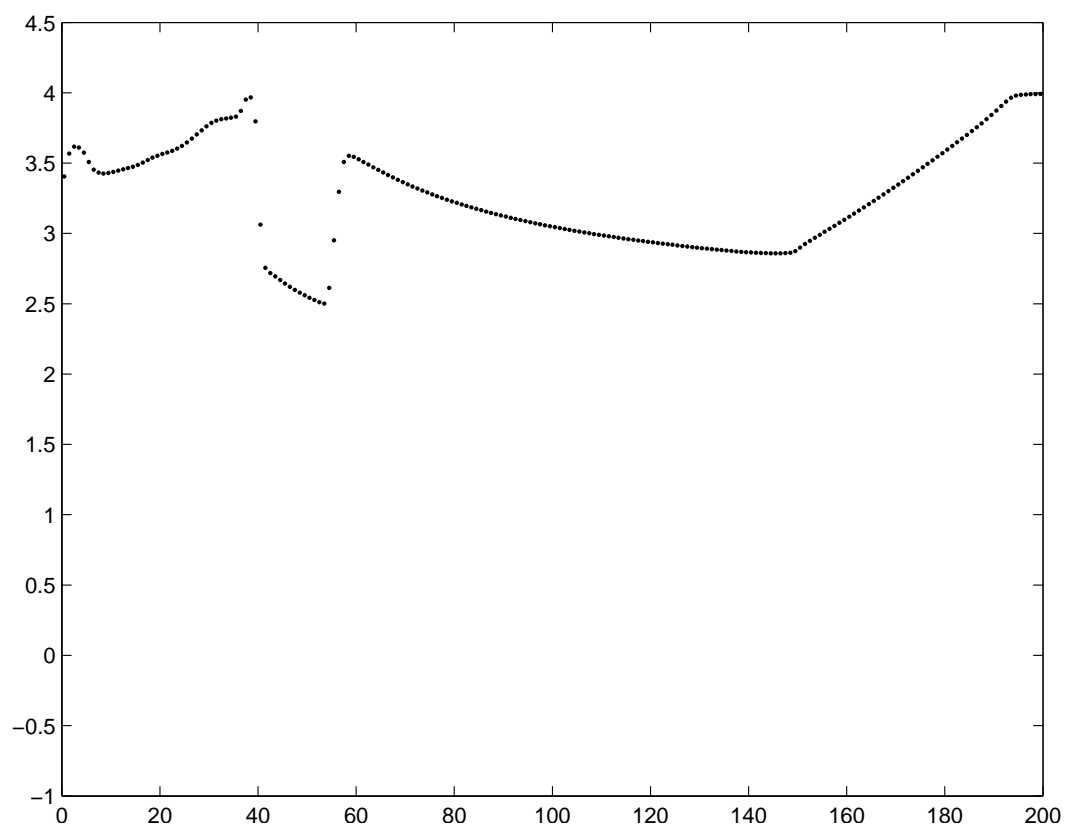


Figure 11: Solution for  $\rho$  using Scheme 2b when  $t = 80$

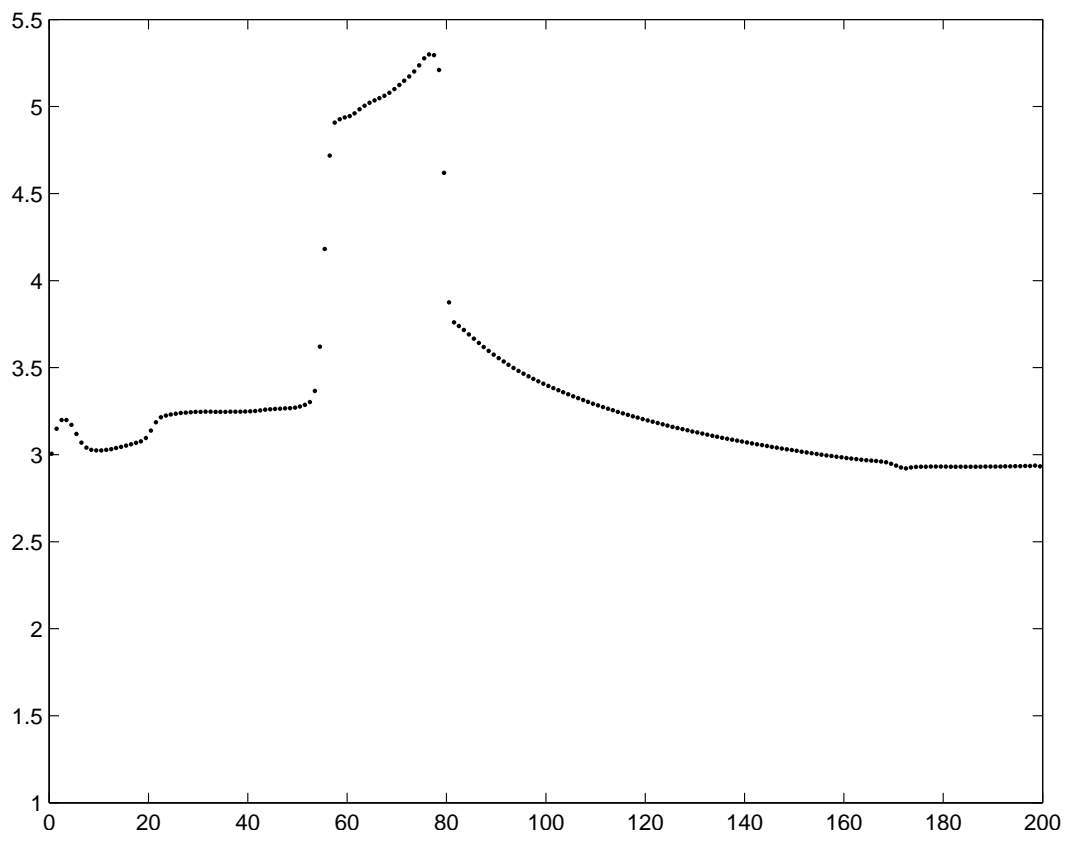


Figure 12: Solution for  $\rho$  using Scheme 2b when  $t = 110$

## References

- [1] P. Glaister., Conservative upwind difference schemes for compressible flows in a Duct. *Computers Math. Applic.* **56**, 1787-1796 (2008).
- [2] P. Glaister., Conservative Upwind Difference Schemes for the Euler Equations for Real Gas Flow in a Duct. *Computers Math. Applic.* **57**, 1432-1437 (2009).

**Received: August 9, 2011**